ISSN:2229-6093

Soham Chakraborty, International Journal of Computer Technology & Applications,Vol 8(6),688-698

POWER SYSTEM STATE ESTIMATION AND OBSERVABILITY ANALYSIS USING ARTIFICIAL NEURAL NETWORKS

Soham Chakraborty
SRM University, Kattankulathur, Chennai

Abstract: *This work proposes a static state estimation method and network observability analysis using artificial neural networks trained using Bayesian Regularization. This method is aimed at reducing computational complexities as in case of conventional method. The proposed method is to be carried out and compared with the conventional weighted least square state estimation algorithm on a system.*

By using ANN based State estimator, it will be a direct procedure unlike WLS method which is a iterative procedure comprising of complex calculations. Here the input and output are mapped in an ANN, so we get direct estimates of state variables given the measurements as input. Hence there is no need to store the huge complex YBUS admittance matrix and perform complex calculations. ANN is implemented to get better and faster results from the state estimator used in load dispatch centres and also smart grids.

Observability Analysis of power system is done prior to running state estimator. If a system is found to be unobservable, then additional meters may have to be placed at particular locations to make the system observable. Network observability analysis identifies the observable islands, unobservable branches and the locations for placement of meters to make the system observable. This work is an iterative procedure and can be done using ANN that will be provide a direct procedure to solve the problem.

Key words: *State Estimation, Weighted Least Square method, Artificial Neural Networks, Numerical Method based on Nodal Variable formulation, Observability Analysis, Measurement Placement to restore observability*

I. INTRODUCTION

State estimation is the process of assigning a value to an unknown system state variable based on measurements from that system according to some criteria. Usually, the process involves imperfect measurements that are redundant, and the process of estimating the system states is based on a statistical criterion that estimates the true value of the state variables to minimize or maximize the selected criterion.

In a power system, the state variables are the voltage magnitudes and relative phase angles at the system nodes. Measurements are required in order to estimate the system performance in real time for both system security control and constraints on economic dispatch.

The inputs to an estimator are imperfect power system measurements of voltage magnitudes and power, VAR, or ampere-flow quantities. The estimator is designed to produce the "best estimate" of the system voltage and phase angles, recognizing that there are errors in the measured quantities and that there may be redundant measurements.

The output data are then used in System Control Centers or Load Dispatching Centre in the implementation of the security-constrained dispatch and control of the system. The best estimates help in maintaining power system monitoring, security, reliability, and proper control of the system.

II. STATE ESTIMATION USING WEIGHTED LEAST SQUARE METHOD

A. Maximum Likelihood Weighted Least-Squares Estimation

a) *The maximum likelihood criterion*, where the objective is to maximize the probability that the estimate of the state variable, $\hat{x}$, is the true value of the state variable vector, $\hat{x}$, (i.e., maximize $P(\hat{x})$=x) [8]**.**

b) *The weighted least-squares criterion*, where the objective is to minimize the sum of the squares of the weighted deviations of the estimated measurements, $\hat{z}$, from the actual measurements, **z [8]**.

c) *The minimum variance criterion*, where the object is to minimize the expected value of the sum of the squares of the deviations of the estimated components of the state variable vector from the corresponding components of the true state variable vector [8].

B. Gaussian or Normal Probability Density Function

If the uncertainties in measured values are plotted as a function of their relative frequency of occurrence, a histogram is obtained to which a continuous curve can be fitted as the number of measurements increases (theoretically, to an infinite number). The continuous curve most commonly encountered is the bell shaped function called the Gaussian or Normal Probability Density Function [6].

ISSN:2229-6093

Soham Chakraborty, International Journal of Computer Technology & Applications,Vol 8(6),688-698

$$p(z) = \frac{1}{\sigma\sqrt{2\pi}} e^{-\frac{1}{2}\left(\frac{z-\mu}{\sigma}\right)^2} \quad (1)$$

z – random variable, μ - mean, σ – standard deviation

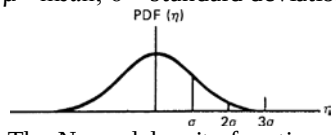

Figure 1: The Normal density function

C. The Likelihood Function

The joint probability density function which represents the probability of measuring m independent measurements, each having the same Gaussian P.D.F can simply be expressed as the product of individual P.D. F's if each measurement is assumed to be independent of the rest.

$$f_m(z)=f(z_1)\, f(z_2)\ldots f(z_m) \quad (2)$$

where z_i : ith measurement, z^T : $[z_1, z_2, \ldots, z_m]$. The function $f_m(z)$ is called the likelihood function for z. It is a measure of the probability of observing the particular set of measurements in the vector z. The objective of the maximum likelihood estimation is to maximize this likelihood function by varying the assumed parameters of the density function, namely its mean and standard deviation [6]. The modified function is called the Log-Likelihood function, $\mathcal{L}$.

$$L = \log fm(z) = \sum_{i=1}^{m} \log f(z_i) = -\frac{1}{2}\sum_{i=1}^{m}\left(\frac{z_i-\mu_i}{\sigma_i}\right)^2 - \frac{m}{2}\log 2\pi - \sum_{i=1}^{m}\log\sigma_i \quad (3)$$

MLE will maximize the likelihood or log-likelihood function for a given set of observations $z_1, z_2, \ldots, z_m$. It can be obtained by solving the following optimization problem and the solution is called the *weighted least square* (WLS) estimator for x.

Maximize $\log fm(z)$

or

Minimize $\sum_{i=1}^{m}\left(\frac{z_i-\mu_i}{\sigma_i}\right)^2$ (4)

or

Minimize $\sum_{i=1}^{m} W_{ii}\, r_i^2$ (5)

subject to $z_i=h_i(x)+r_i,\ i=1,2,\ldots m$

here $W_{ii}=\sigma_i^{-2}$, $r_i=z_i-\mu_i$

D. Measurement Model

$$z = \begin{bmatrix} z_1 \\ z_2 \\ \vdots \\ z_m \end{bmatrix} = \begin{bmatrix} h_1(x_1,x_2,\ldots,x_m) \\ h_2(x_1,x_2,\ldots,x_m) \\ \vdots \\ h_m(x_1,x_2,\ldots,x_m) \end{bmatrix} + \begin{bmatrix} e_1 \\ e_2 \\ \vdots \\ e_m \end{bmatrix} = h(x) + e \quad (6)$$

here $h_i(x)$ is the nonlinear function relating measurement i to the state vectors $x_1, x_2, \ldots, x_m$ and $e_1, e_2, \ldots, e_m$ are the measurement errors.

Assumptions: $E(e_i)=0$ and measurement errors are independent, i.e. $E\{e_ie_j\}=0$, hence *Covariance* $(e)=E\{e.e^T\}=R=\text{diag}\{\sigma_1^2, \sigma_2^2, \ldots, \sigma_m^2\}$.

The WLS estimator will minimize the following objective function:

$$J(x) = \sum_{i=1}^{m}\frac{(z_i-h_i(x))^2}{R_{ii}} = [z-h(x)]^T R^{-1}[z-h(x)] \quad (7)$$

At the minimum, the first order optimality conditions will have to be satisfied.

$$g(x) = \frac{\partial J(x)}{\partial x} = -H^T R^{-1}[z-h(x)] = 0 \quad (8)$$

where $H(x) = \left[\frac{\partial h(x)}{\partial x}\right]$ is the Jacobian matrix

Expanding the nonlinear function $g(x)$ into its Taylor series around the state vector x^k yields:

$$g(x)=g(x^k)+G(x^k)(x-x^k)+\ldots=0$$

Neglecting the higher order terms leads to an iterative solution scheme known as the Gauss-Newton method as shown below (k – iteration index):

$$x^{k+1}=x^k-[G(x^k)]^{-1}.g(x^k)$$

$$G(x^k) = \left[\frac{\partial g(x^k)}{\partial x}\right] = H^T(x^k).R^{-1}.H(x^k) \quad (9)$$

$G(x)$ is called the Gain matrix. It is sparse, positive-definite, symmetric provided that the system is fully observable.

$$G(x^k)\Delta x^{k+1} = H^T(x^k).R^{-1}.[z-h(x^k)] \quad (10)$$

E. WLS Algorithm

The iterative solution algorithm for WLS state estimation problem can be outlined as follows [6]:

1. The iterations are started with iteration index k=0.
2. The state vector x^k is initialized as a flat start.
3. The gain matrix is calculated, $G(x^k) = H^T(x^k).R^{-1}.H(x^k)$.
4. The inverse of gain matrix is determined by obtaining the adjoint matrix and dividing it by the determinant and so $\Delta x^{k+1} = G(x^k)^{-1}H^T(x^k).R^{-1}.[z-h(x^k)]$.
   (Generally gain matrix is decomposed into Cholesky factors $G=L.L^T$ and forward/backward substitution is performed to obtain Δx^{k+1}).
5. Convergence criterion is tested max $|\Delta x^{k+1}| < \epsilon$
6. If no, update $x^{k+1}=x^k+\Delta x^k$, $k=k+1$, and go to step 3, Else stop.

F. The Measurement Function

Most commonly used measurements are the line power flows, bus power injections, bus voltage magnitudes and line current flow magnitudes. These measurements can be expressed using state variables using rectangular or polar coordinates. When using polar coordinates for a system containing N buses, we have 2N-1 state variables, N bus voltages and N-1 phase angles, with the phase angle of reference bus is set equal to an arbitrary value, such as 0. The state vector x will have the following form assuming bus 1 is chosen as the reference:

$$x^T=[\theta_2\ \theta_3 \ldots\ \theta_N V_1\ V_2 \ldots V_N]$$

Assuming a two-port π model for the network branches, the expressions for different types of measurements are given below.

ISSN:2229-6093

Soham Chakraborty, International Journal of Computer Technology & Applications,Vol 8(6),688-698

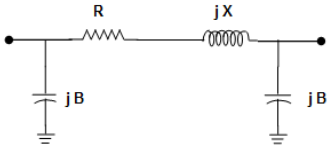

Figure 2: Two port pi model of a network branch

- Real and Reactive power injection at bus i:

$$P_i = V_i \sum_{j\in Ni} V_j\left(G_{ij}\cos\theta_{ij} + B_{ij}\sin\theta_{ij}\right) \quad (11)$$

$$Q_i = V_i \sum_{j\in Ni} V_j\left(G_{ij}\sin\theta_{ij} - B_{ij}cos\theta_{ij}\right) \quad (12)$$

- Real and Reactive power flow from bus i to bus j:

$$P_{ij} = V_i^2(g_{si} + g_{ij}) - V_iV_j\left(g_{ij}\cos\theta_{ij} + b_{ij}\sin\theta_{ij}\right) \quad (13)$$

$$Q_{ij} = V_i^2(b_{si} + b_{ij}) - V_iV_j\left(g_{ij}\sin\theta_{ij} - b_{ij}\cos\theta_{ij}\right) \quad (14)$$

- Line current flow magnitude from bus i to j:

$$\frac{\sqrt{P_{ij}^2 + Q_{ij}^2}}{V_i}$$

or ignoring the shunt admittance (g_{si}+jb_{si}):

$$\sqrt{(g_{ij}^2 + b_{ij}^2)(V_i^2 + V_j^2 - 2V_iV_j\,cos\theta_{ij})} \quad (15)$$

where V_i , θ_i are the voltage magnitude and phase angle at bus i.
$\theta_{ij} = \theta_i - \theta_j$.
G_{ij}+B_{ij} is the ij[th] element of the complex bus admittance matrix.
g_{ij}+b_{ij} is the admittance of the series branch connecting buses i and j.
g_{sj}+b_{sj} is the admittance of the shunt branch connected at bus shown in figure 3.2.
Ni is the *set* of buses connected directly to bus i.

G. *The Measurement Jacobian, H*

The basic structure of the Jacobian matrix is as follows:

$$H = \begin{bmatrix} \frac{\partial P_{inj}}{\partial\theta} & \frac{\partial P_{inj}}{\partial V} \\ \frac{\partial P_{flow}}{\partial\theta} & \frac{\partial P_{flow}}{\partial V} \\ \frac{\partial Q_{inj}}{\partial\theta} & \frac{\partial Q_{inj}}{\partial V} \\ \frac{\partial Q_{flow}}{\partial\theta} & \frac{\partial Q_{flow}}{\partial V} \\ \frac{\partial I_{mag}}{\partial\theta} & \frac{\partial I_{mag}}{\partial V} \\ 0 & \frac{\partial V_{mag}}{\partial V} \end{bmatrix} \quad (16)$$

- Elements corresponding to real power injection measurements:

$$\frac{\partial P_i}{\partial\theta_i} = \sum_{j=1}^{N} V_iV_j\left(-G_{ij}\sin\theta_{ij} + B_{ij}\cos\theta_{ij}\right) - V_i^2B_{ii} \quad (17)$$

$$\frac{\partial P_i}{\partial\theta_j} = V_iV_j\left(G_{ij}\sin\theta_{ij} - B_{ij}\cos\theta_{ij}\right) \quad (18)$$

$$\frac{\partial P_i}{\partial V_i} = \sum_{j=1}^{N} V_j\left(G_{ij}\cos\theta_{ij} + B_{ij}\sin\theta_{ij}\right) + V_iG_{ii} \quad (19)$$

$$\frac{\partial P_i}{\partial V_j} = V_i\left(G_{ij}\cos\theta_{ij} + B_{ij}\sin\theta_{ij}\right) \quad (20)$$

- Elements corresponding to reactive power injection measurements:

$$\frac{\partial Q_i}{\partial\theta_i} = \sum_{j=1}^{N} V_iV_j\left(G_{ij}\cos\theta_{ij} + B_{ij}\sin\theta_{ij}\right) - V_i^2GB_{ii} \quad (21)$$

$$\frac{\partial Q_i}{\partial\theta_j} = V_iV_j\left(-G_{ij}\cos\theta_{ij} - B_{ij}\sin\theta_{ij}\right) \quad (22)$$

$$\frac{\partial Q_i}{\partial V_i} = \sum_{j=1}^{N} V_j\left(G_{ij}\sin\theta_{ij} - B_{ij}\sin\theta_{ij}\right) - V_iG_{ii} \quad (23)$$

$$\frac{\partial Q_i}{\partial V_j} = V_i\left(G_{ij}\sin\theta_{ij} - B_{ij}\cos\theta_{ij}\right) \quad (24)$$

- Elements corresponding to real power flow measurements:

$$\frac{\partial P_{ij}}{\partial\theta_i} = V_iV_j\left(g_{ij}\sin\theta_{ij} - b_{ij}\cos\theta_{ij}\right) \quad (25)$$

$$\frac{\partial P_{ij}}{\partial\theta_j} = -V_iV_j\left(g_{ij}\sin\theta_{ij} - b_{ij}\cos\theta_{ij}\right) \quad (26)$$

$$\frac{\partial P_{ij}}{\partial V_i} = -V_j\left(g_{ij}\cos\theta_{ij} + b_{ij}\sin\theta_{ij}\right) + 2V_i\left(g_{si} + g_{ij}\right) \quad (27)$$

$$\frac{\partial P_{ij}}{\partial V_j} = -V_i\left(g_{ij}\cos\theta_{ij} + b_{ij}\sin\theta_{ij}\right) \quad (28)$$

- Elements corresponding to reactive power flow measurements:

$$\frac{\partial Q_{ij}}{\partial\theta_i} = -V_iV_j\left(g_{ij}\cos\theta_{ij} + b_{ij}\sin\theta_{ij}\right) \quad (29)$$

$$\frac{\partial Q_{ij}}{\partial\theta_j} = V_iV_j\left(g_{ij}\cos\theta_{ij} + b_{ij}\sin\theta_{ij}\right) \quad (30)$$

$$\frac{\partial Q_{ij}}{\partial V_i} = -V_j\left(g_{ij}\sin\theta_{ij} - b_{ij}\cos\theta_{ij}\right) - 2V_i\left(b_{ij} + b_{si}\right) \quad (31)$$

$$\frac{\partial Q_{ij}}{\partial V_j} = -V_i\left(g_{ij}\sin\theta_{ij} - b_{ij}\cos\theta_{ij}\right) \quad (32)$$

- Elements corresponding to voltage magnitude measurements:

$$\frac{\partial V_i}{\partial V_i} = 1,\ \frac{\partial V_i}{\partial V_j} = 1,\ \frac{\partial V_i}{\partial\theta_i} = 0, \frac{\partial V_i}{\partial\theta_i} = 1 \quad (33)$$

- Elements corresponding to current magnitude measurements (ignoring the shunt admittance of the branch):

$$\frac{\partial I_{ij}}{\partial\theta_i} = \frac{g_{ij}^2 + b_{ij}^2}{I_{ij}} V_iV_jsin\theta_{ij} \quad (34)$$

$$\frac{\partial I_{ij}}{\partial\theta_j} = -\frac{g_{ij}^2 + b_{ij}^2}{I_{ij}} V_iV_jsin\theta_{ij} \quad (35)$$

$$\frac{\partial I_{ij}}{\partial V_i} = \frac{g_{ij}^2 + b_{ij}^2}{I_{ij}} (V_i - V_jcos\theta_{ij}) \quad (36)$$

$$\frac{\partial I_{ij}}{\partial V_j} = \frac{g_{ij}^2 + b_{ij}^2}{I_{ij}} (V_j - V_icos\theta_{ij}) \quad (37)$$

III. NETWORK OBSERVABILITY ANALYSIS

A. *Introduction*

Power system state estimator uses the set of available measurements in order to estimate the system state. Given a set of measurements and their locations, the network observability analysis will determine if a unique estimate can be found for the system state. This analysis may be carried out off-line during the initial phase of a state estimator installation, in order to check the adequacy of the existing measurement configuration. If the system is found not to be observable, then additional meters may have to be placed at particular locations. Observability analysis is also done on-

ISSN:2229-6093

line, prior to running the state estimator. Network observability analysis identifies all the observable islands, unobservable branches, and locations for placement of meters to make the system observable. Temporary unobservability may occur due to telecommunication failure [6].

B. Network Observability Using Numerical Method Based On the Nodal Variable Formulation

Numerical observability analysis can also be carried out by using the nodal variables. Nodal variable vector is denoted by *x* and represents the vector of magnitude and phase angle of all bus voltages in the system [6]. Consider the linearized measurement model, where measurement errors are ignored due to their irrelevance in the observability analysis.

Using the weak coupling between P - V and Q - δ, the linearized model can be decoupled as:

$$\Delta z_A = H_{AA}\Delta\theta \quad and \quad \Delta z_R = H_{RR}\Delta V \tag{38}$$

$\Delta z_A, \Delta z_R$ is the real and reactive power measurement mismatch vectors respectively.

$H_{AA} = \frac{\partial h_A}{\partial \theta}$ is the decoupled Jacobian for the real power measurements.

$H_{RR} = \frac{\partial h_R}{\partial V}$ is the decoupled Jacobian for the reactive power measurements.

$\Delta\theta = \theta - \theta_0$ and $\Delta V = V - V_0$

Assuming that the P, Q measurements come in pairs, P - θ and Q - V observability can be separately tested. Note that, unlike θ, the voltage solution requires a measured reference bus. Hence, following the P - θ analysis, it should be further checked to ensure that at least one voltage measurement exists per observable island. A network is said to be P - θ observable if the rank of matrix $H_{P\theta}$ is equal to N-1. Also, network is said to be $Q - V$ observable if the rank of the H_{QV} matrix is equal to N.

It should be noted that the system observability is independent of the branch parameters as well as the operating state of the system. So, all system branches can be assumed to have an impedance of jl.0 p.u. and all bus voltages can be set equal to 1.0 p.u. for the purpose of observability analysis. Then, the d.c. power flows along these system branches can be written as:

$$P_b = A\theta \tag{39}$$

where P_b is the vector of branch flows, A is the branch-bus incidence matrix, θ is the vector of bus voltage phase angles.

If the estimated state $\hat{\theta}$ is zero, then all branch flows will be zero as given by Equation (39). Using the DC measurement model: $z_A = H_{AA}\theta$, the WLS estimate for θ will be given by: $\hat{\theta}=G_{AA}^{-1}t_A$

A null estimate for $\hat{\theta}$ will be obtained for an observable system when all system measurements Δz_A, i.e. flows and injection measurements, are all zero. If there exists an estimate $\hat{\theta}$ which satisfies the measurement equation Z_A=0, yet yields a non-zero branch flow $P_b \neq 0$, $\hat{\theta}$ will be called an unobservable state. Furthermore, those branches carrying nonzero flows, will be referred to as unobservable branches.

C. Identification of Observable Islands

This procedure needs to be carried out recursively, each time eliminating the irrelevant injections until all observable islands are identified. Irrelevant injections are those that are incident to unobservable branches. The algorithm is given below.

1. All irrelevant branches are eliminated. These are branches that have no incident measurements.
2. Form the decoupled linearized gain matrix for the P – δ estimation problem: $G_{AA} = H_{AA}^T H_{AA}$.
3. G_{AA} is factorized by modifying the zero pivots and the right side vector as described above. The state variables are determined and then the branch flows are found.
4. All unobservable branches and all injections that are incident to these unobservable branches are identified and eliminated.
5. If no more unobservable branches are found in step 4, then the observable islands are determined separated by the unobservable branches and stopped. Else considering the modified network, go to step 2.

D. Measurement Placement to restore Observability

Once the observable islands are identified, measurements can be added to merge these islands so that eventually a single observable island can be formed. The candidate measurements that can merge islands are:

- the line flows along branches that connect observable islands, and
- the injection at the boundary buses of observable islands.

The following measurement placement algorithm can then be implemented based on the above defined matrices:

1. Form the gain matrix (from $G = H^T H$) and compute the factor matrix L. Modify the matrix L with diagonal elements as 1.
2. Since $G = L D L^T$ diagonal matrix $D = L^{-1} G (L^{-1})^T$. Check whether D has only one zero pivot. If yes, stop, the system is observable.
3. Else assemble W matrix from the rows of L^{-1} matrix corresponding to zero pivot positions.
4. Form the candidate measurement list. The list will contain flow and injection measurements incident to branches connecting observable islands, which have already been identified by the observability analysis.
5. Build the measurement Jacobian H_c for the candidate measurements.
6. Compute $B = H_c W^T$. Obtain the reduced row echelon form of B as E. The linearly independent rows of E will correspond to all the measurements required to be placed.

ISSN:2229-6093

Soham Chakraborty, International Journal of Computer Technology & Applications,Vol 8(6),688-698

IV. ARTIFICIAL NEURAL NETWORK

A. ANN Configuration

The ANN's elemental unit is the mathematical neuron, which receives a fraction w of the input data x, simplified by a bias b, and processes the information according to its activation function F [1].

$$y = F(n) = F\left(\sum_j w_j . x_j + b\right) \quad (39)$$

Neural networks are known to be universal approximators for any non-linear function and they are generally used for mapping error tolerant problems that have much data trained in noise. A neural network consists of many layers namely: an input layer, a number of hidden layers and an output layer. The input layer and the hidden layer are connected by synaptic links called weights and likewise the hidden layer and output layer also have connection weights. When more than one hidden layer exists, weights exist between such layers. Neural networks use some sort of "learning" rule by which the connections weights are determined in order to minimize the error between the neural network output and desired output.

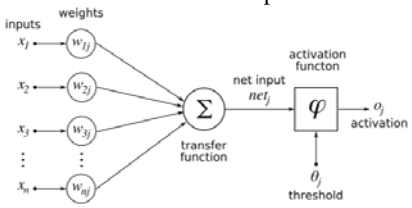

Figure 3: Basic Layout of ANN

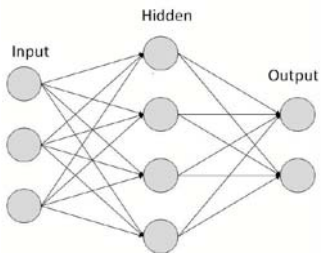

Figure 4: Multi Layered ANN

B. Polynomial Curve Fitting

The problem is to fit a polynomial to a set of N data points by the technique of minimizing an error function [7]. Considering the M^{th} order polynomial given by

$$y(x) = w_0 + w_1 x + \ldots + w_m x^m = \sum_{j=0}^{m} w_j . x^j \quad (40)$$

This can be regarded as a non-linear mapping which takes x as input and produces y as output. The precise form of the function $y(x)$ is determined by the values of the parameters $w_0, \ldots, w_m$, which are analogous to the weights in a neural network.

The desired outputs y for a specific input x^n is called target values t^n. In order to find the suitable values for the coefficients in the polynomial, it is convenient to consider the error between the desired output t^n, for a particular input x^n and the corresponding value predicted by the polynomial function given by $y(x^n;w)$. Standard curve fitting procedures involve minimizing the square of this error, summed over all data points, or mean squared error, given by

$$E = \frac{1}{N} \sum_{n=1}^{N} \{(x^n; w) - t^n\}^2 \quad (41)$$

In order to assess the capability of the polynomial to generalize to new data, it is convenient to consider the root mean square (RMS) error given by

$$E^{RMS} = \sqrt{\frac{1}{N} \sum_{n=1}^{N} \{(x^n; w) - t^n\}^2} \quad (42)$$

C. Bayesian Learning of Network Weights

The Bayesian approach considers a probability distribution function over weight space, representing the relative degrees of belief in different values for the weight vector. Once the data has been observed, it can be converted to a posterior distribution through the use of Bayes' theorem and can be used to evaluate the predictions of the trained network for new values of the input variables [7]. In the Bayesian framework, we consider a probability distribution over a weight values. In the absence of any data, this is described by a prior distribution which we shall denote by $p(w)$. Here $w = (w_0, \ldots w_M)$ denotes vector of adaptive weight (and bias) parameters. Let the target data from the training set be denoted by $D = (t^1,\ldots,t^N)$. Once we observe the data D we can write down an expression for the posterior probability distribution for the weights, which we denote by $p(w|D)$, using Bayes' theorem.

$$p(w/D) = \frac{p(w/D)p(w)}{p(D)} \quad (43)$$

The normal objective function is the Mean Squared Error (MSE) function.

V. ANN BASED STATE ESTIMATOR AND OBSERVABILITY ANALYSIS

The ANN is trained to perform a nonlinear mapping between input measurements and output state variables and other estimated measurements. Once the ANN is trained, state estimation is a direct procedure, without having the need of going through the iterative procedure of WLS method that consumes a lot a computational memory. Also, Y_{BUS} matrix is also not required to be stored. Thus ANN saves time, computational burden reduced [1].

In case of observability analysis, ANN is trained with various patterns of input measurements [3]. In this case the inputs are the locations of measurements available in the system. If an input is available at a particular location, injections or flows, 1 is taken as an input to the ANN, and if it's not available, then input to the ANN is 0. The output of the ANN is the locations of the measurement placement to restore observability of the system. Flow measurements are the candidate measurements here. So the outputs of the ANN are the branches where measurement placement is to be done. If

ISSN:2229-6093

output is 1 for a branch, then that branch needs a measurement to be placed, and if its 0, measurement is not placed there.

VI. RESULTS OF STATE ESTIMATOR

A. *State Estimation using WLS and ANN SE*

Given the network and the required bus data, the true bus voltages and line flows are determined by Conventional Load Flow using Newton Raphson method. Given the meter placement, type and accuracies, a set of meter readings is simulated by adding errors from a random number generator, which generates a number based on Gaussian density function with the mean value and standard deviation specified. Using the simulated measurements, the best estimates of bus voltages and phase angles are calculated using the Weighted Least Square State Estimator. State estimation is also done using ANN. The percentage error in the estimates with respect to the true values are determined. This is done for IEEE 5 bus, 30 bus, 118 bus system.

B. *IEEE 5 Bus System State Estimation*

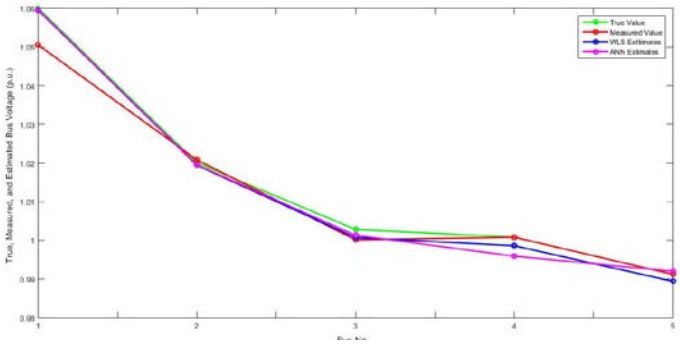

Figure 5: True, Measured, Estimated Bus Voltage (p.u.) for IEEE 5 Bus System

The plot shows that the estimated voltage is close enough to the true value, with marginal difference for both WLS & ANN estimated values.

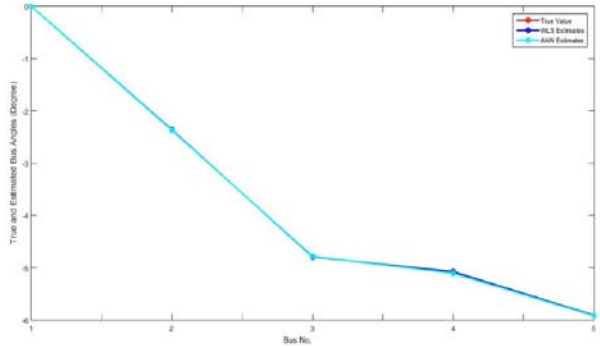

Figure 6: True and Estimated Bus Angles (Degree) for IEEE 5 Bus System

The estimated angles are close enough to the true values and almost coinciding with the true values (both WLS and ANN estimates)

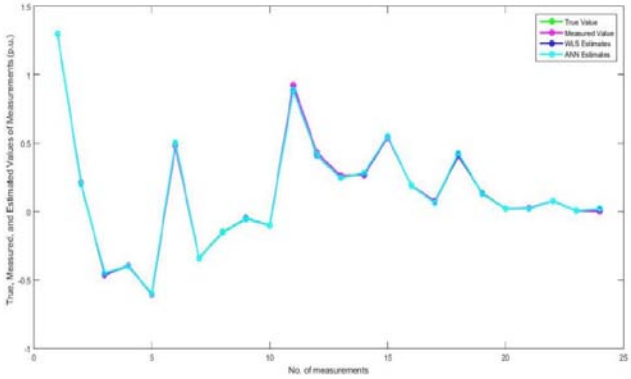

Figure 7: True. Measured and Estimated values of power injections and power flows (p.u.) for IEEE 5 Bus System

The plot shows that the estimated values are close enough to the true value, with minor difference for both WLS & ANN estimated values.

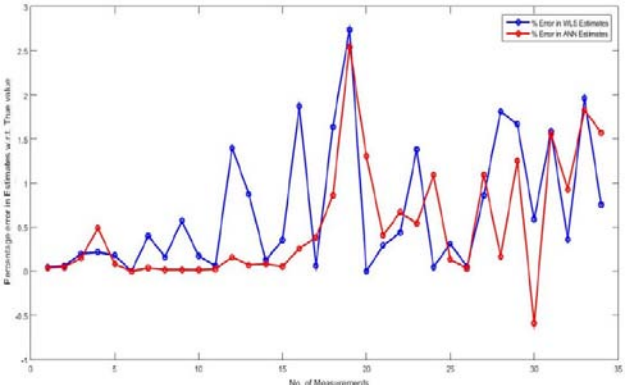

Figure 8: Percentage error in different estimates w.r.t. true value for IEEE 5 Bus System

It is evident from the above plot that ANN estimates have better accuracy than WLS estimates in some cases, and equal accuracies for the rest.

ISSN:2229-6093

C. IEEE 30 Bus System State Estimation

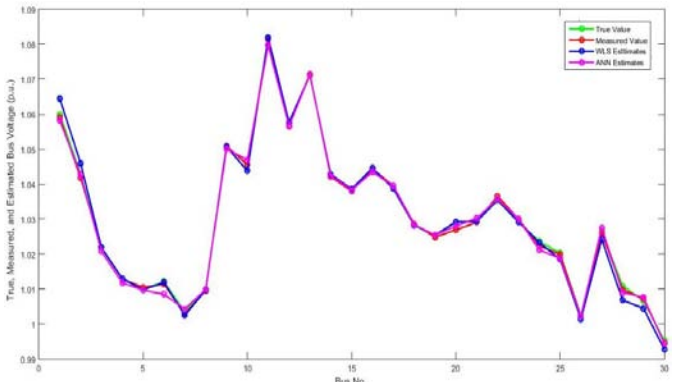

Figure 9: True, Measured and Estimated Bus Voltages (p.u.) for IEEE 30 Bus System

The plot shows that both WLS and ANN estimates show nearly equal accuracy close enough to true value.

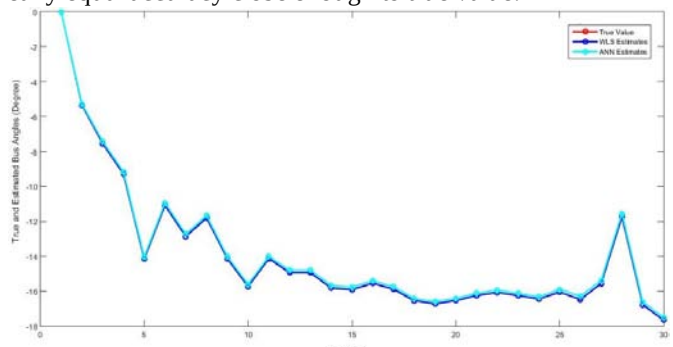

Figure 10: True and Estimated Values of Bus Angles (Degree) for IEEE 30 Bus system

The plot shows that the estimated angles are almost coinciding the true value (both WLS, ANN).

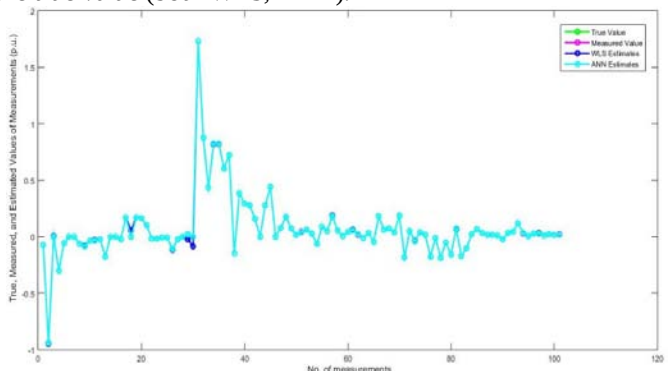

Figure 11: True, Measured, and Estimated Values of power injections and power flows measurements (p.u.)for IEEE 30 Bus system

The ANN estimates have almost equal accuracies or better accuracies than the WLS estimates

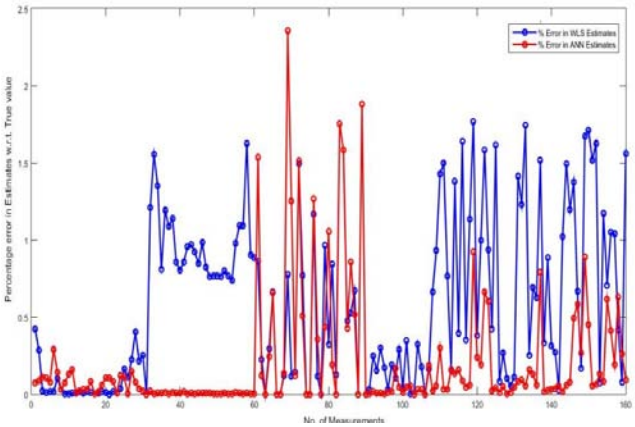

Figure 12: Percentage error in estimated measurements w.r.t. true values

It's clear from the above plot ANN performs much better than WLS in some cases, and have almost equal accuracies in other instances

D. IEEE 118 Bus System State Estimation

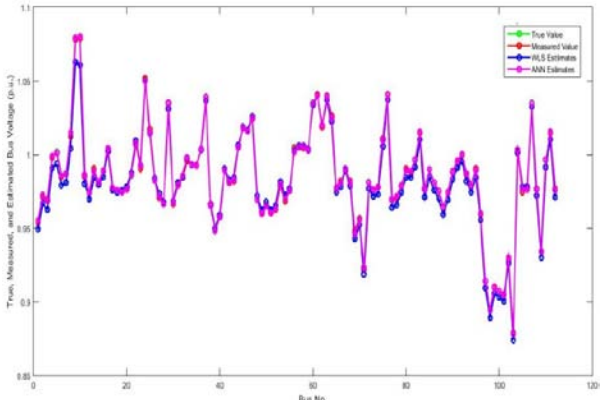

Figure 13: True, Measured and Estimated Bus Voltages (p.u.) for IEEE 118 Bus System

The plot shows that both WLS, ANN estimates show nearly equal accuracy.

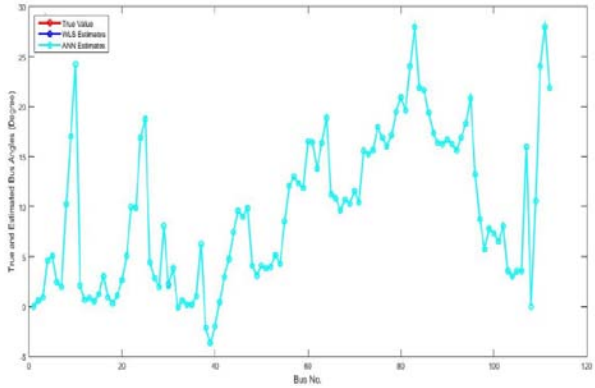

Figure 14: True and Estimated Bus Angles for IEEE 118 Bus System

ISSN:2229-6093

Soham Chakraborty, International Journal of Computer Technology & Applications,Vol 8(6),688-698

ANN & WLS estimates coincide with the true values of bus angles with equal accuracy.

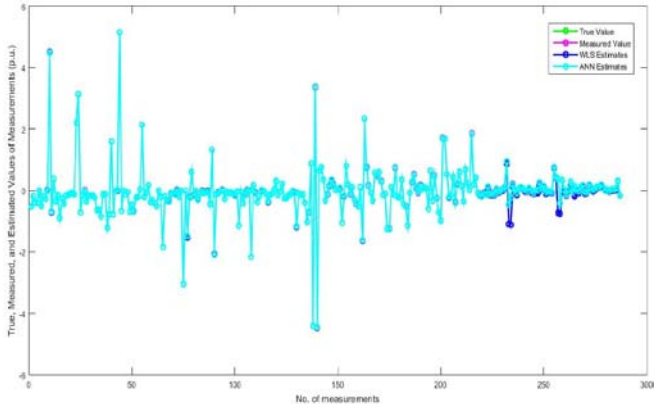

Figure 15: True, Measured, and Estimated values of power injections, power flows measurements (p.u.) for IEEE 118 Bus System

ANN shows better accuracy in a few instance, but both have equal accuracies elsewhere.

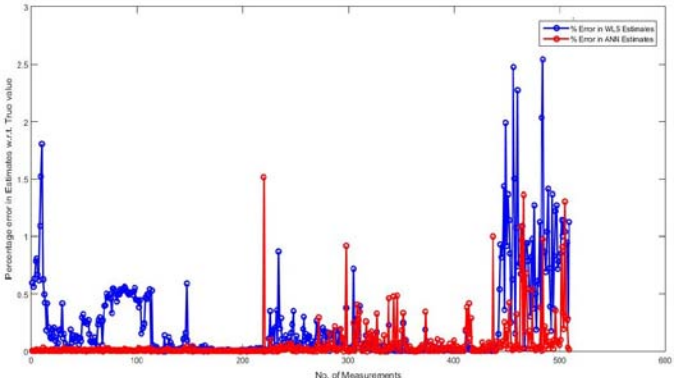

Figure 16: Percentage error in different measurements w.r.t. true value for IEEE 118 Bus System

The error encountered in ANN SE is lower than WLS SE in most cases, though WLS shows better accuracy in the other cases.

E. Mean Squared Error Plots of ANN Based SE

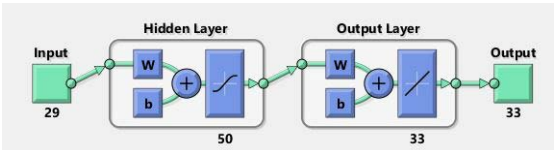

Figure 17: ANN SE Configuration for IEEE 5 Bus System

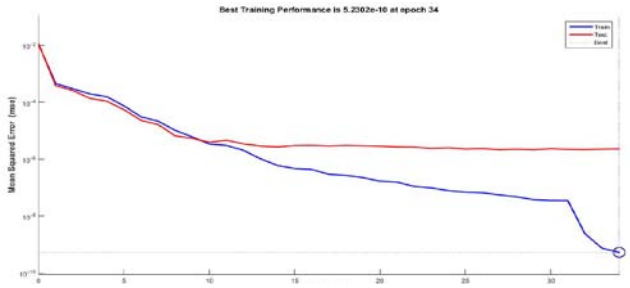

Figure 18: MSE 5.2302e-10 at epoch 34 for IEEE 5 Bus System

The MSE is very low, and shows that the ANN outputs are close enough to the targets specified.

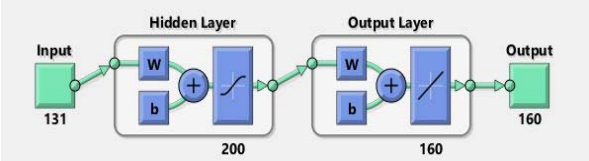

Figure 19: ANN SE Configuration for IEEE 30 Bus System

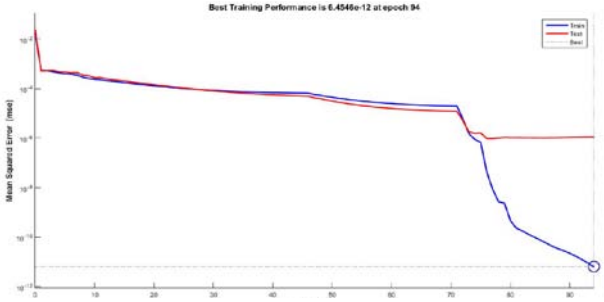

Figure 20: MSE 6.4545e-12 at epoch 94 for IEEE 30 Bus System

The MSE is very low, and shows that the ANN outputs are close enough to the targets specified.

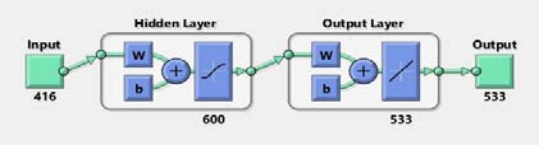

Figure 21: ANN SE Configuration for IEEE 118 Bus System

ISSN:2229-6093

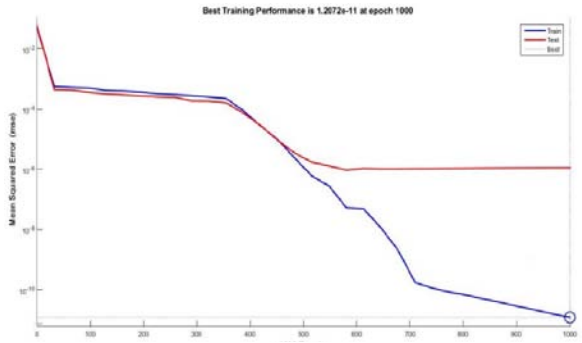

Figure 22: MSE 1.2672e-11 at epoch 1000 for IEEE 118 Bus System

The MSE is very low, and shows that the ANN outputs are close enough to the targets specified.

VII. Observability Analysis Using Numerical Method Based On The Nodal Variable Formulation And ANN

A. IEEE 5 Bus System Observability Analysis

Measurements Present:
Power Injection at bus: 1, 2. Line Flows: 1-2, 2-3

Unobservable branches: 2-4, 2-5, 3-4, 4-5

Placement of line flows measurements to restore observability: 4-5
ANN output for measurement placement: 0.85 (for 4-5)

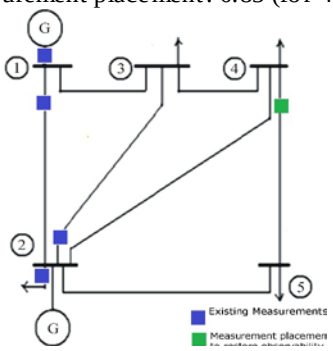

Figure 23: IEEE 5 BUS SYSTEM SLD WITH MEASUREMENTS POSITIONS

B. IEEE 5 Bus System Observability Analysis

Measurements Present:
Power Injection at bus: 1, 2, 3, 4, 5, 6, 9, 13, 14, 15, 18, 21, 23, 24, 25, 27, 28, 29, 30.
Line Flows: 1-2, 3-4, 6-7, 6-8, 9-11, 4-12, 12-13, 14-15, 10-21, 10-22, 15-23, 24-25,25-26, 28-27, 27-30, 29-30, 8-28, 6-28

Unobservable branches: 12-16, 16-17, 19-20, 10-20, 10-17

Placement of line flows measurements to restore observability: 12-16, 16-17, 19-20
ANN output for measurement placement: 0.92 (for 12-16), 0.799 (for 16-17), 0.82 (for 19-20)

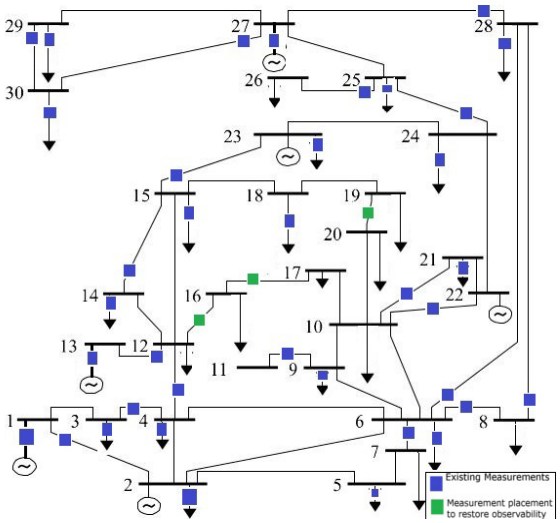

Figure 24: IEEE 30 Bus System SLD with measurement positions

C. IEEE 118 Bus System Observability Analysis

Measurements Present:
Power Injection at bus: 1, 2, 4, 5, 8, 9, 10, 12, 13, 15, 18, 19, 20, 21, 23, 24, 25, 26, 27, 29, 31, 36, 37, 39, 43, 44, 48, 49, 50, 52, 53, 57, 59, 61, 63, 64, 65, 66, 67, 71, 73, 75, 79, 82, 83, 84, 85, 87, 88, 90, 93, 94, 95, 97, 102, 104, 106, 108, 109, 110,114,116,117,118
Line Flows: 3-5, 6-7, 8-9, 8-5, 11-12, 3-12, 14-15, 12-16, 15-17, 17-18, 18-19, 15-19,28-29, 30-17, 29-31, 27-32, 34-36, 34-37, 38-37, 39-40, 43-44, 34-43, 44-45, 46-47,47-49,42-49, 49-50, 49-51, 52-53, 53-54, 55-56, 56-57, 50-57,56-58, 51-58, 56-59,56-59, 59-60, 59-61,60-61, 60-62, 61-62, 64-65, 65-68, 68-69, 69-70, 71-73, 70-75,69-75, 78-79, 79-80, 81-80, 77-82, 83-84, 85-86, 86-87, 85-88, 89-90, 89-90, 89-92,92-93,92-94, 93-94, 94-96, 80-98, 92-100, 95-96, 96-97, 98-100, 99-100, 92-102,100-104,103-104,100-106,104-105, 105-106, 105-107, 105-108, 106-107, 109-110,32-113, 32-114, 27-115, 12-117

Unobservable branches: 22-23, 23-24, 23-25, 26-25, 25-27, 27-28, 26-30, 17-31, 23-32, 31-32, 40-41, 41-42, 24-70, 70-71, 24-72, 71-72, 70-74, 74-75, 76-77, 69-77, 75-77, 68-81, 110-111, 110-112, 17-113, 75-118, 76-118

Placement of line flows measurements to restore observability: 110-111, 68-81, 24-72, 76-77, 22-23
ANN output for measurement placement: 0.86, 0.76, 0.91, 0.88, 0.96 respectively.

ISSN:2229-6093

D. Mean Squared Error Plots of ANN Based Observability Analysis

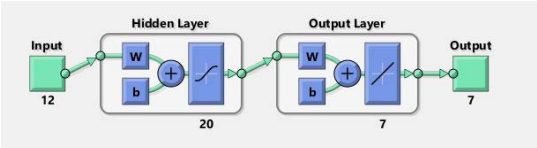

Figure 25: ANN OA configuration for IEEE 5 Bus system

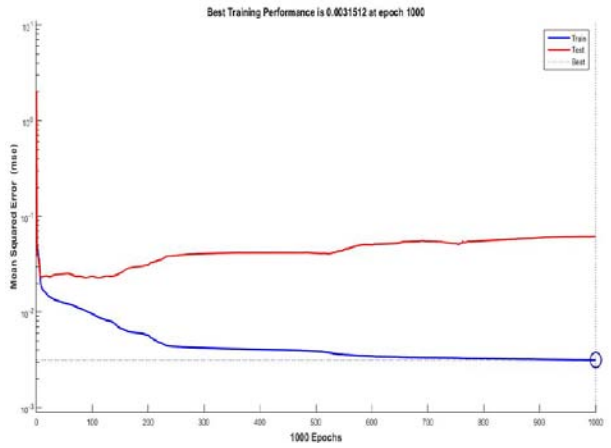

Figure 26: MSE 0.0031512 at epoch 1000 for IEEE 5 Bus system

The MSE is low, and shows that the ANN outputs tend to reach the targets specified.

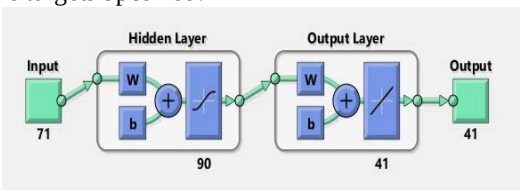

Figure 27: ANN OA Configuration for IEEE 30 Bus System

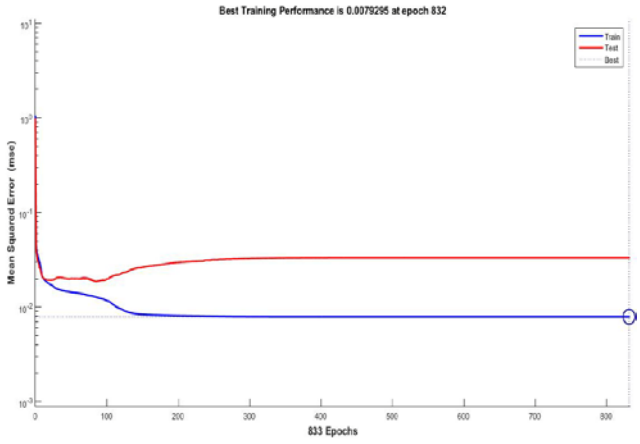

Figure 28: MSE 0.0079295 at epoch 832 for IEEE 30 Bus system

The MSE is low, and shows that the ANN outputs tend to reach the targets specified.

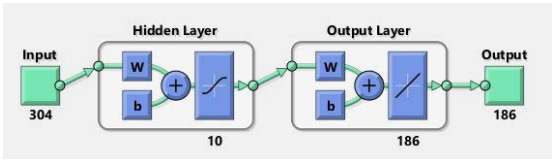

Figure 29: ANN OA configuration for IEEE 118 system bus

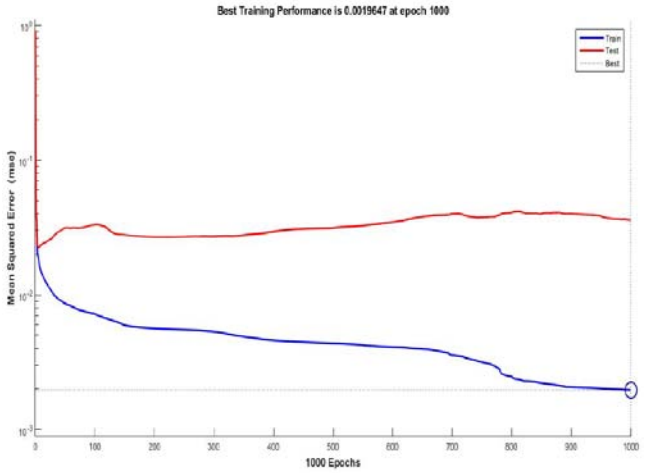

Figure 30: MSE 0.0019647 at epoch 1000 for IEEE 118 bus system

The MSE is low, and shows that the ANN outputs tend to reach the targets specified.

VIII. CONCLUSION

This work proposes incorporation of ANN based state estimator at load dispatch centres and energy control centres, to get faster results, in a direct process avoiding the complex iterative process of WLS method. The ANNs are trained with some patterns and tested with patterns which were not used for training and their performance is at an acceptable range.

Incorporating neural networks will reduce computational complexities involved in the iterative procedures. It is a direct process, with inputs and outputs mapped. It responds fast, saves time and computational burdens are reduced.

ANN based state estimator is found to perform better than WLS state estimator in some cases, and in other times it shows same accuracy as the WLS estimator. The process will involve lesser error than WLS method, with reduced complexities in calculations. Also it will give proper results with lesser number of inputs compared to WLS method. In this context, we dealt with IEEE 5, 30 ,118 Bus Systems and got acceptable results.

This work has proposed a new method based on artificial neural network to perform observability analysis and measurement placement to restore observability. This method gives good results if ANN is trained with large number of patterns.

Observability analysis and State Estimation using ANN should be tested for larger power systems with FACTS devices and PMU measurements in future. It should be trained with adequate number of patterns to produce proper results and reduce mean squared error to a value as low as possible.

APPENDIX

Estimated Values of State Variables for IEEE 5 Bus System

BUS	True Volt. (P.U.)	Measd Volt. (P.U.)	WLS Estmd Volt.	ANN Estmd Volt.	%Error (WLS Estmd. Volt.)	%Error (ANN Estmd. Volt.)
1	1.0600	1.0505	1.0595	1.0596	0.0462	0.0377
2	1.0200	1.0208	1.0194	1.0195	0.0612	0.0490
3	1.0028	1.0001	1.0007	1.0013	0.1999	0.1496
4	1.0008	1.0008	0.9986	0.9959	0.2161	0.4896
5	0.9912	0.9912	0.9894	0.9920	0.1802	0.0807

True Angle (Deg.)	WLS Estmd Angle	ANN Estmd.Angle	%Error (WLS Estmd. Angle)	%Error (ANN Estmd. Angle)
0.00	0.00	0.00	-	-
-2.373	-2.364	-2.372	0.4018	0.0363
-4.783	-4.791	-4.782	0.1619	0.0180
-5.108	-5.0788	-5.107	0.5702	0.0169
-5.920	-5.9098	-5.919	0.1759	0.0146

Estimated Values of State Variables for IEEE 30 Bus System

BUS	True Volt. (P.U.)	Measd Volt. (P.U.)	WLS Estmd Volt.	ANN Estmd Volt.	%Error (WLS Estmd. Volt.)	%Error (ANN Estmd. Volt.)
1	1.0600	1.0591	1.0645	1.0583	0.4230	0.0743
2	1.0430	1.0418	1.0460	1.0427	0.2871	0.0853
3	1.0217	1.0219	1.0219	1.0208	0.0208	0.1122
4	1.0129	1.0129	1.0130	1.0118	0.0104	0.1055
5	1.0100	1.0105	1.0098	1.0097	0.0162	0.0801
6	1.0121	1.0114	1.0119	1.0085	0.0161	0.2911
7	1.0035	1.0029	1.0025	1.0043	0.1021	0.1434
8	1.0100	1.0096	1.0097	1.0099	0.0310	0.0322
9	1.0507	1.0509	1.0507	1.0501	0.0045	0.0718
10	1.0438	1.0455	1.0438	1.0469	0.0040	0.1311
11	1.0820	1.0814	1.0819	1.0797	0.0069	0.1583
12	1.0576	1.0567	1.0577	1.0566	0.0055	0.0097
13	1.0710	1.0715	1.0712	1.0713	0.0153	0.0225
14	1.0429	1.0421	1.0428	1.0424	0.0073	0.0306
15	1.0384	1.0380	1.0386	1.0383	0.0152	0.0301
16	1.0445	1.0444	1.0446	1.0435	0.0096	0.0828
17	1.0387	1.0395	1.0387	1.0395	0.0030	0.0029
18	1.0282	1.0286	1.0283	1.0284	0.0081	0.0160
19	1.0252	1.0248	1.0254	1.0254	0.0182	0.0613
20	1.0291	1.0269	1.0292	1.0280	0.0106	0.1065
21	1.0293	1.0291	1.0293	1.0302	0.0000	0.1078
22	1.0353	1.0366	1.0355	1.0357	0.0161	0.0833
23	1.0291	1.0300	1.0292	1.0301	0.0086	0.0075
24	1.0237	1.0224	1.0233	1.0212	0.0343	0.1188
25	1.0202	1.0199	1.0185	1.0188	0.1645	0.1092
26	1.0025	1.0023	1.0014	1.0023	0.1099	0.0007
27	1.0265	1.0260	1.0242	1.0275	0.2252	0.1494
28	1.0109	1.0098	1.0068	1.0090	0.4012	0.0762
29	1.0067	1.0073	1.0045	1.0077	0.2153	0.0369
30	0.9953	0.9946	0.9928	0.9944	0.2517	0.0227

REFERENCES

[1] Ovidiu Ivanov and Mihai Gavrilaş Power System Department, Electrical Engineering, Energetics and Applied Informatics Faculty "Gheorghe Asachi" Technical University Iasi, Romania "State Estimation with Neural Networks and PMU Voltage Measurements" International *Conference and Exposition on Electrical and Power engineering (EPE 2014)*, pp. 983-988 16-18 October 2014, Iasi, Romania.

[2] Efthymios Manitsas, Member, IEEE, Ravindra Singh, Member, IEEE, Bikash C. Pal, Senior Member, IEEE, and Goran Strbac, Member, IEEE "Distribution System State Estimation Using an Artificial Neural Network Approach for Pseudo Measurement Modeling" *IEEE transactions on power systems*, vol. 27, no. 4, pp. 1888-1896 November 2012.

[3] Amit Jain, R. Balasubramanian, Senior Member, IEEE, S. C. Tripathy, Brij N. Singh, Member, IEEE, and Yoshiyuki Kawazoe "Power System Topological Observability Analysis Using Artificial Neural Networks" *IEEE transactions on power systems* pp. 1-6 2005.

[4] O.AlsaG, N. Vempati, B. Stott PCA Corporation Mesa, Arizona, USA ,A. Monticelli UN ICAMP Campinas, SP, Brazil "Generalized State Estimation" *IEEE Transactions on Power Systems*, Vol. 13, No. 3, pp. 1069-1075 August 1998

[5] N. Yadaiah,∗MIEEE,G. Sowmya JNTU "Neural Network Based State Estimation of Dynamical Systems" 2006 *International Joint Conference on Neural Networks* Sheraton Vancouver Wall Centre Hotel, Vancouver, BC, Canada pp. 1042-1049 July 16-21, 2006

[6] Ali Abur, Antonio Gomez Exposito, "Power system state estimation, theory and implementation" MARCEL *DEKKER, INC.*

[7] Christopher M.Bishop "Neural Networks for Pattern Recognition" *Clarendon Press Oxford*

[8] Allen J.Wood, Bruce F. Wollenberg, Geral B. Sheble, "Power Generation, Operation, and Control", *Wiley*